

RALAD: Bridging the Real-to-Sim Domain Gap in Autonomous Driving with Retrieval-Augmented Learning

Jiacheng Zuo^{*,1}, Haibo Hu^{*,2}, Zikang Zhou², Yufei Cui³, Ziquan Liu⁴,
Jianping Wang², Nan Guan², Jin Wang^{†,1}, Chun Jason Xue⁵

Abstract—In the pursuit of robust autonomous driving systems, models trained on real-world datasets often struggle to adapt to new environments, particularly when confronted with corner cases such as extreme weather conditions. Collecting these corner cases in the real world is non-trivial, which necessitates the use of simulators for validation. However, the high computational cost and the domain gap in data distribution have hindered the seamless transition between real and simulated driving scenarios. To tackle this challenge, we propose Retrieval-Augmented Learning for Autonomous Driving (RALAD), a novel framework designed to bridge the real-to-sim gap at a low cost. RALAD features three primary designs, including (1) domain adaptation via an enhanced Optimal Transport (OT) method that accounts for both individual and grouped image distances, (2) a simple and unified framework that can be applied to various models, and (3) efficient fine-tuning techniques that freeze the computationally expensive layers while maintaining robustness. Experimental results demonstrate that RALAD compensates for the performance degradation in simulated environments while maintaining accuracy in real-world scenarios across three different models. Taking Cross View as an example, the mIOU and mAP metrics in real-world scenarios remain stable before and after RALAD fine-tuning, while in simulated environments, the mIOU and mAP metrics are improved by 10.30% and 12.29%, respectively. Moreover, the re-training cost of our approach is reduced by approximately 88.1%. Our code is available at <https://github.com/JiachengZuo/RALAD.git>.

I. INTRODUCTION

As the application of machine learning in autonomous driving continues to gain unstoppable momentum [1], a vast array of models has emerged for solving various autonomous driving tasks [2], [3], [4], including image segmentation [5], [6], [7], object detection [8], [9], and motion planning [10]. These models are usually trained and tested using real-world datasets such as KITTI [11], Waymo [12], and nuScenes [13], which cover common driving scenarios. However, autonomous driving systems inevitably encounter corner cases, such as extreme weather conditions, unexpected pedestrian behavior, and rare road scenarios, which challenge

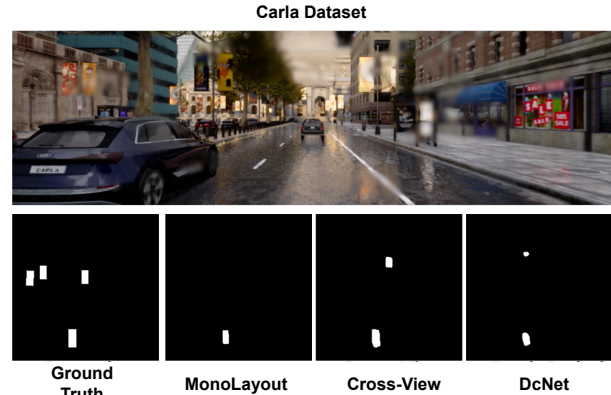


Fig. 1. The performance of baseline models in CARLA: All models exhibit varying degrees of performance degradation in 3D object detection.

their perception and decision-making capabilities [14], [15]. Given the high safety standards required in vehicle operation to prevent life-threatening accidents, it is imperative that autonomous systems rigorously address and test these corner cases to ensure robust performance [14], [15]. Models trained on real-world datasets predominantly encounter regular driving scenarios, making it challenging to cover and address the rare and complex corner cases [21], [16], [19]. To replicate and test corner cases, simulators are often used, as real-world data is difficult to collect [21]. Models trained on real-world datasets cannot be directly applied in simulators because of the gap between real and simulated environments, as shown in Figure 1 and Table I, where we tested three models (Monolayout [5], Cross-View [6], and DcNet [7]) in CARLA, resulting in significant decreases in both performance and accuracy. With the advent of large models, the cost and time required for model training have significantly increased [4]. Therefore, finding cost-effective methods to improve model performance in simulators has become a major challenge.

We found that in the field of computer vision (CV), there are already methods that utilize nearest neighbor search and feature fusion for domain adaptation to address cross-domain dataset problems [16], [18]. Our problem can also be regarded as a cross-domain problem between real datasets and simulated datasets. Given the similarity between their problem and ours, we attempt to apply this method to autonomous driving. However, applying this method to autonomous driving needs to face three major challenges. Firstly, the significant differences between images in other fields and autonomous driving images hinder the direct use of this method in this field, as autonomous driving needs to

*Equal contribution †Corresponding author
¹Department of Computer Science, Soochow University. jczuo102137@stu.suda.edu.cn, wjin1985@suda.edu.cn
²Department of Computer Science, City University of Hong Kong. {haibohu2-c, zikanzhou2-c}@my.cityu.edu.hk, {nanguan, jianwang}@cityu.edu.hk
³Department of Computer Science, McGill University. yufeicui92@gmail.com
⁴School of Electronic Engineering and Computer Science, Queen Mary University of London. ziquan.liu@qmul.ac.uk
⁵Department of Computer Science, Mohamed bin Zayed University of Artificial Intelligence. jason.xue@mbzuai.ac.ae

consider both the direct distance between individual images and the group distance between image sets. Secondly, unlike imaging that completely uses real data, simulated images are completely different from real images. We do not know the best granularity for calculating similarity in simulated data. Finally, it is crucial to meet the need for low-cost training while ensuring the robustness and reliability of the model.

To address these challenges, we propose Retrieval-Augmented Learning for Autonomous Driving (RALAD). To handle the gap between real and simulated images in autonomous driving, we introduce the optimal transport method that considers both individual and group distances. For the unknown optimal granularity in simulated data, we adjust the optimal transport from object-level to pixel-level retrieval. Finally, we adopt a fine-tuning approach by freezing computationally expensive neural network layers and re-training only selected layers, which reduces computational costs while maintaining model robustness and reliability in low-cost training environments. We selected three 3D object detection models for our experiments, as 3D object detection is one of the most critical tasks in autonomous driving. Conducting experiments in this domain provides the strongest justification for evaluating the effectiveness of our approach.

Our contributions are summarized as follows:

- We introduce RALAD, a framework that addresses the real-to-sim gap in autonomous driving and provides pixel-level OT capabilities.
- We apply RALAD to three models, achieving significant performance improvements.
- We establish a mapping between real and simulated environments and conduct extensive experiments to validate the approach.

In the following, we discuss the related work in Section II and detail the RALAD framework in Section III, with Section IV presenting the experimental results and Section V concluding the paper.

II. RELATED WORK

A. Retrieval-Augmented Learning

Retrieval-Augmented Learning (RAL) is an approach that enhances learning models, it integrates retrieval mechanisms to leverage existing data representations, thereby improving performance and efficiency. For example, Yottixel [22] employs a mix of supervised and unsupervised methods, including segmentation, clustering, and deep networks, to analyze image patches and employ distance metrics for efficient search and retrieval. SISH [23] utilizes a tree structure for rapid WSI search and an uncertainty-based ranking for retrieval, reducing storage and labeling by building on preprocessed mosaics without pixel or ROI labels, using self-supervised learning indices and pre-trained embeddings. HHOT [24] introduces optimal transport (OT) as a metric for comparing whole slide images (WSIs) or across WSI datasets, theoretically underpinning the application of OT for steering the retrieval and assembly of datasets. In RAM-MIL [18], the attention weight serves as a measure of

probability density, signifying the "mass" being transferred. By quantifying this, the method computes the conversion cost across various data domains. It then employs this distribution for nearest-neighbor retrieval, seamlessly integrating features from distinct domains to address out-of-domain challenges.

B. Gap Between Real And Sim

In the field of autonomous driving, there exists the issue of the Gap during the application process from simulation to reality [25], where discrepancies in lighting, textures, vehicle dynamics, and agent behaviors between virtual and real environments complicate the direct application of simulation results. To address this, researchers have developed two primary approaches: sim2real knowledge transfer and the use of digital twins (DTs) [17], [28]. In knowledge transfer learning for autonomous driving, the RG problem is compounded by uneven environmental sampling and complex physical parameters [26]. To overcome this, researchers have developed strategies such as curriculum learning, meta-learning, knowledge distillation, robust reinforcement learning, domain randomization, and transfer learning [27]. Domain randomization, in particular, helps align simulation parameters with real-world variability, facilitating the transfer of learned strategies to real-world applications. Conversely, digital twin technology creates virtual models of real-world entities or systems. A case in point is the development of the SynFog dataset [28], which uses an end-to-end simulation process to produce photo-realistic synthetic fog data, enhancing learning-based algorithm research and facilitating the model's transition from synthetic to real data. Nonetheless, despite their promise, these methods confront the issue of high computational expenses, particularly in complex, dynamic real-world settings.

C. 3D Object Detection In Autonomous Driving

3D object detection is crucial for autonomous driving as it enables vehicles to accurately perceive and understand their surroundings, which is essential for safe navigation and decision-making. Conventionally, this has been achieved with the help of LiDAR sensors, which, although precise, are prohibitively expensive and computationally demanding. To address these limitations, the field has seen a significant advancement with the application of deep learning techniques that leverage monocular cameras for 3D detection. Specifically, the development of bird's-eye view (BEV) representations from monocular images has emerged as a promising and more cost-effective alternative. Techniques such as MonoLayout [5] and Cross View [6] demonstrate the potential of using these BEV representations to perform 3D object detection. Cross View, in particular, has introduced a cross-view transformation module and a context-aware discriminator to enhance results, achieving cutting-edge performance in vehicle occupancy estimation. Nonetheless, issues such as class imbalance and low computational efficiency remain. The Dual-Cycled Cross-View Transformer network (DcNet) [7] has been proposed to tackle these challenges by integrating focal loss and optimizing multi-class learning,

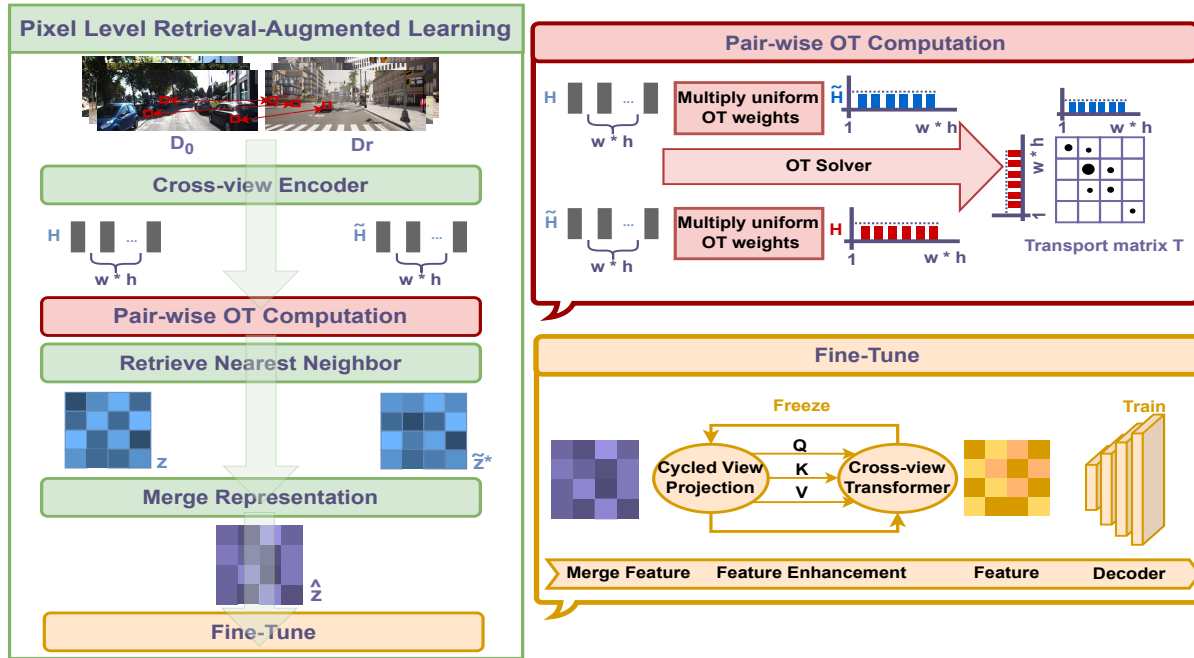


Fig. 2. The left panel shows the pixel-level retrieval enhancement process: feature extraction by an Encoder, OT algorithm for transport cost calculation, nearest neighbor retrieval, feature fusion, and fine-tuning. The top right details the OT computation process. The bottom right explains fine-tuning with fused features, freezing all but the Decoder layers.

setting new standards of performance in the field of 3D object detection for autonomous driving.

III. METHOD

This section provides a detailed explanation of the RALAD framework, as shown in Figure 2. We introduce Pixel-Level Retrieval-Augmented Learning based on Optimal Transport into autonomous driving, using Cross-view as an example to illustrate the RALAD process.

A. Problem Formulation

The gap between real-world and simulation (real2sim) primarily arises from the cross-domain challenges between real and simulated data in autonomous driving. To address this, we consider two datasets: the Real dataset D_r and the Sim dataset D_s . The Real dataset is defined as $D_r = \{X_n, Y_n\}_{n=1}^{N_r}$, where N_r is the number of images, and the Sim dataset is $D_s = \{\tilde{X}_m, \tilde{Y}_m\}_{m=1}^{N_s}$, with N_s being the number of simulated images. To bridge the gap between these two datasets, the first step is to establish a mapping relationship between them. We extract features from real and simulated images using an encoder function $g(\cdot)$, resulting in $H_k = g(x_k)$ for real images and $\tilde{H}_k = g(\tilde{x}_k)$ for simulated images, where x_k and \tilde{x}_k are individual images from X and \tilde{X} , respectively. The features H_k and \tilde{H}_k are composed of pixel-wise feature vectors, with $H_k = \{h_i\}_{i=1}^{w \cdot h}$ and $\tilde{H}_k = \{\tilde{h}_i\}_{i=1}^{w \cdot h}$, where h_i and \tilde{h}_i represent the feature vectors of pixel i in the real and simulated images, respectively. Our ultimate goal is to identify the similarity between H_k and \tilde{H}_k , thereby enabling cross-domain retrieval between the two datasets.

B. Pixel-Level Retrieval-Augmented Learning based on Optimal Transport in Real2Sim

To address the mapping relationship between features from different domains, we introduce Retrieval-Augmented Learning based on Optimal Transport. However, previous RAL approaches were primarily object-level and focused on real-world images. Given the cross-domain nature of our real and simulated environments, simple object-level approaches are insufficient for effectively establishing relationships between real and simulated images. Therefore, pixel-level computations are required to ensure fine-grained matching between real and virtual images. This precise matching aids in identifying and preserving detailed information, thereby establishing a more accurate correspondence between the two domains.

Furthermore, previous RAM based on OT was applied to simple classification tasks, whereas our autonomous driving BEV perception task is far more complex. To address this challenge, we propose to treat every pixel as a sample in the OT computation, while each image is treated as a probability distribution. We assign uniform weights to all instances and leave the non-uniform OT calculation to future exploration. The purpose of the OT algorithm is to calculate the distance between two features H_n (real-world) and \tilde{H}_m (simulation) for subsequent retrieval of the nearest feature. The formula is as follows:

$$d_{\text{OT}}(H_n, \tilde{H}_m) = \sum_{i=1}^{w \cdot h} c(h_i, \tilde{h}_i) T_{ii} + \beta \cdot \sum_i T_{ii} \log T_{ii}$$

$$\text{s.t. } T^T \mathbf{1}_{w \cdot h} = H_n, T \mathbf{1}_{w \cdot h} = \tilde{H}_m, T \geq 0. \quad (1)$$

In this equation, T denotes the transport plan matrix where

each element T_{ii} specifies the amount of "mass" to be transported from h_i to \tilde{h}_i . The function $c(h_i, \tilde{h}_i)$ is a cost function that quantifies the cost of transporting a unit of mass from h_i to \tilde{h}_i . A common choice of $c(h_i, \tilde{h}_i)$ is the squared l_2 distance between the features, i.e., $c(h_i, \tilde{h}_i) = \|h_i - \tilde{h}_i\|_2^2$, here, $1_{w \cdot h}$ is vector of ones. We also introduced entropy regularization [29] to reduce sensitivity to outlier instances.

Subsequently, the nearest neighbor feature for H_n would be one \tilde{H}_i in the CARLA dataset, which we define as \tilde{H}^* . Both H_n and \tilde{H}^* are then utilized for the subsequent process of feature merge. The formulation is as follows:

$$\tilde{H}^* = \min \sum_{i=1}^{N_s} d_{\text{OT}}(H_n, \tilde{H}_i) \quad (2)$$

C. Convex Merge and Fine-Tune

In the feature retrieval phase of autonomous driving, we have already obtained it through OT computed the optimal matching simulated feature \tilde{H}^* . Upon finding this match, we employ a convex merge operation to combine the real feature H with the simulated feature \tilde{H}^* , resulting in a new composite feature \hat{H} , calculated as $\hat{H} = \pi(H, \tilde{H}^*)$. The merging function $\pi(\cdot)$ is typically a convex combination method. The set of merged features denoted as $D_m = \{\hat{H}_i\}_{i=1}^{N_m}$, with N_m being the number of features, is then utilized for the fine-tuning phase, aimed at enhancing the model's ability to generalize from simulated to real data. The fine-tuning process is governed by the following loss function, which is consistent with the one used in Cross_view [6]:

$$\mathcal{L} = \mathcal{L}_{BCE} + \lambda \mathcal{L}_{\text{cycle}} + \beta (\mathcal{L}_1^D + \mathcal{L}_2^D) \quad (3)$$

During fine-tuning, we maintain the integrity of the pre-trained model by freezing all layers except for the decoder, which allows for the adaptation of the model to the new combined feature set without overwriting the learned representations.

IV. EXPERIMENT

To evaluate the effectiveness of the proposed RALAD method, which improves recognition of real-world scenes using simulated data and bridges the gap between simulated and real-world environments, we employed a multi-dataset approach involving KITTI, CARLA datasets, and other real-world images. This method allows for a comprehensive evaluation of the performance of RALAD. The experimental process begins with an overview of the implementation and dataset details, followed by the experimental results of our method, and demonstrate the performance of RALAD retrieval and its applications in BEV perception. Finally, we show the influence of the convex combination ratio on the model's performance during fine-tuning.

A. Dataset and Metrics

The workstation used for this task was equipped with a single NVIDIA RTX A4000 GPU card. All the input images are normalized to 1024×1024 and the output size is 256×256 . The network parameters are randomly initialized and

we adopt the Adam optimizer [29] and use a mini-batch size of 6. The initial learning rate is set to 1×10^{-4} , and it is decayed by 0.1 after 25 epochs.









The KITTI dataset comprises 7481 monocular images from vehicle front cameras, split into 3712 training and 3769 validation images based on Chen et al.'s 3D object detection criteria, with ground truth derived from [5]. For the CARLA dataset, collected via the CARLA 0.9.15 software with robust annotation features, we gathered data from maps like Town01, Town02, and Town07, comprising 500 training, 473 validation, and 227 test images, totaling 1200. Utilizing the RALAD algorithm, we extracted 4066 features from the KITTI and CARLA training sets and fine-tuned the pre-trained Cross View model on KITTI. The 4066 extracted features were allocated to training (2536) and validation (1530) sets. We then assessed the fine-tuned model on both datasets to showcase its real-world and simulated performance, using Mean Intersection over Union (mIOU) and Mean Precision (mAP) as metrics.

B. Experimental Results

We conducted comprehensive experiments using the KITTI and CARLA datasets. To ensure the generalization of RALAD, we selected three models (MonoLayout, Cross View, and DcNet) that are highly regarded in the field of 3D object detection. Detailed experiments were performed on both the original models and their RALAD fine-tuned counterparts in a consistent hardware and software environment.

Metrics Results: Our experimental metrics are shown in Table I, which shows the performance of three models is compared with and without RALAD fine-tuning on KITTI (real-world) and CARLA (simulation) datasets. For MonoLayout, RALAD shows minimal improvement on the KITTI dataset (mIOU from 30.18% to 30.26%, with a slight mAP decrease from 45.91% to 44.98%). However, on the CARLA dataset, it achieves significant improvements (mIOU from 25.26% to 34.13%, mAP from 48.93% to 56.41%). This suggests that RALAD helps more in simulation environments, particularly for this model. For Cross View, the gains on KITTI are modest (mIOU from 38.85% to 39.21%, mAP from 56.64% to 56.49%), while on CARLA, the improvements are much more pronounced (mIOU from 30.55% to 40.82%, mAP from 53.25% to 65.54%). For DcNet, the improvements on KITTI are slight (mIOU from 39.44% to 39.07%, mAP from 58.89% to 57.64%), but the model benefits greatly from RALAD on CARLA (mIOU from 31.09% to 42.11%, mAP from 54.72% to 67.24%). These results suggest that RALAD has a more substantial impact on the simulation dataset, improving both detection accuracy and precision.

Training Overhead: Our RALAD adopts the fine-tuning approach, which can reduce the time cost of re-training existing models, as shown in Table II. To compare the performance of RALAD fine-tuning with standard model re-training, we conducted experiments using 1200 features in a consistent environment. For Cross View, the original model requires 41.54 seconds per epoch on KITTI and 41.33

	KITTI 1	CARLA 1 (Best Match)	CARLA 2	CARLA 3
Group 1				
Group 2				

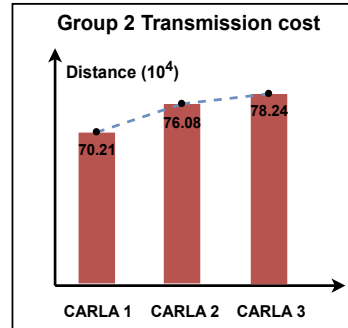
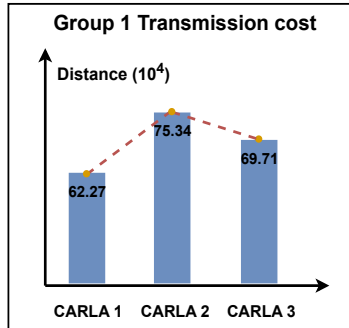


Fig. 3. The table displays two sets of nearest neighbor results for KITTI 1, with these results drawn from the CARLA dataset. CARLA 1 stands out as the optimal match for KITTI 1 among the retrieved neighbors. Below the table, a pair of bar graphs illustrate the transmission cost comparison between KITTI 1 and the CARLA features, a lower transmission cost indicates a higher degree of similarity between the images.

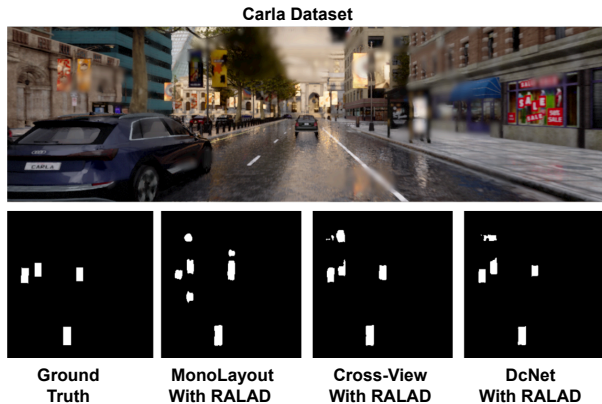


Fig. 4. **The performance of models with RALAD in CARLA:** All models show varying degrees of performance improvement in 3D object detection

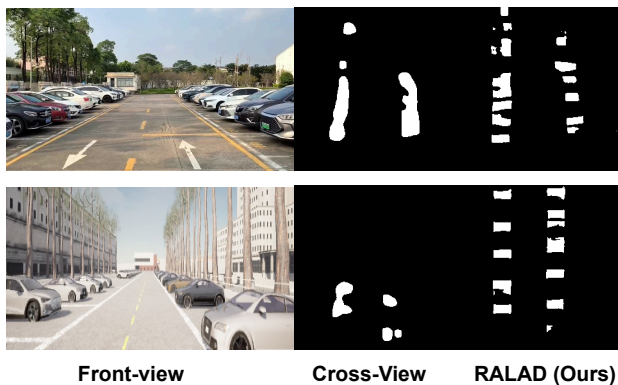


Fig. 5. Evaluation in the real world. **Center:** the compared baseline (Cross_view). **Right:** the baseline enhanced by RALAD (RALAD.Cross_view).

seconds on CARLA in re-train, while RALAD fine-tuning only needs 5.27 seconds on KITTI and 5.29 seconds on CARLA. In comparison, MonoLayout and DcNet also show significant reductions in training time with RALAD, from 34.84 to 3.81 seconds on KITTI and from 68.07 to 20.23 seconds, respectively. These results highlight RALAD’s efficiency, especially for large-scale adaptation.

Visualizations: To further demonstrate the improvements of RALAD on the CARLA dataset, we re-tested the scene from Figure 1, as shown in Figure 4. There is a significant improvement in detecting vehicles in close-range scenes, especially with DcNet, which successfully identifies vehicles entirely. For distant scenes, there is a qualitative leap in detection, almost matching the ground truth. Given the unique characteristics of real and virtual environments, we reconstructed a nearly identical mapping of the real-world scene in CARLA to minimize external factors. Visualizations were conducted to illustrate the improvements RALAD offers over the original models in the same scenarios. We collected parking lot data using our autonomous vehicle equipped with the open-source Autoware. Universe autonomous driving system for testing. The same positions and parking lot scenarios were recreated in CARLA for comparison. As shown in Figure 5, the fine-tuned models with RALAD provide more accurate vehicle detection in both real and virtual environments when compared to the original BEV perception images. We synthesized the comparison dataset into the video.

C. OT Improves The Performance

In this section, we conducted experiments to validate the effectiveness of our OT algorithm in computing the similarity between real-world and virtual-world feature maps. As shown in Figure 3, the algorithm successfully retrieves the most approximate feature map from each dataset. Specifically, a lower OT distance indicates a higher degree of similarity between two feature maps, such as those from KITTI1 and CARLA1 in Group 1 and Group 2. Both groups demonstrate high consistency in key features (e.g., vehicle positions and lane conditions) and achieve the minimum required transmission costs of 62.27×10^4 and 70.21×10^4 , respectively. These results highlight the capability of our pixel-level OT algorithm to accurately compute the similarity between feature maps in practical applications, enabling effective matching of real and virtual data. The findings are consistent with our proposed theory, confirming the enhanced performance of the improved OT algorithm in similarity calculations, thereby providing a solid foundation for subsequent feature fusion and model training.

D. BEV Perception Domain Adaptation

Our RALAD framework is designed to meet the requirements of BEV perception tasks directly and efficiently. When addressing BEV perception, RALAD performs precise feature matching in the target domain, accurately mapping the source and target domains. It retrieves the feature representation most similar to each feature in the source domain, ensuring a high degree of correspondence between the two domains. As shown in Figure 3, this consistency is demonstrated between the KITTI 1 and Carla 1 groups. Subsequently, we leverage these fused feature representations and integrate spatial information from both the source and target domains to fine-tune the final decoder. By adopting a pixel-level OT strategy, this approach achieves cross-domain alignment within the BEV instance space, taking advantage of geometric structures. This strategy significantly improves pixel-level alignment accuracy between the source and target domains, effectively transferring discriminative information from the source domain to the target domain through the feature fusion process. As a result, the model learns more generalized feature representations, enhancing its generalization ability and robustness across different scenarios.

E. Convex Combination Ratio

A core aspect of our RALAD framework is the fusion of features extracted from real and virtual data. Different fusion ratios can yield significantly varied results for the model. To explore this, we conducted comparison experiments using four different ratio settings, based on a total of 1800 features. We tested the following combinations of KITTI to CARLA: 0.7:0.3, 0.6:0.4, 0.5:0.5, and 0.4:0.6. As shown in Table III, For the 0.6:0.4 combination, the model achieved a balanced performance, slightly decreasing on KITTI (32.10% mIOU, 54.02% mAP) but showing a substantial improvement on CARLA (35.12% mIOU, 63.33% mAP), making it an optimal trade-off between real and simulated data. In contrast,

TABLE I
MODEL PERFORMANCE ON KITTI AND CARLA

Methods	KITTI		CARLA	
	mIOU(%)	mAP(%)	mIOU(%)	mAP(%)
MonoLayout [5]	30.18	45.91	25.26	48.93
MonoLayout+RALAD (ours)	30.26	44.98	34.13 ↑	56.41 ↑
Cross_view [6]	38.85	56.64	30.55	53.25
Cross_view+RALAD (ours)	39.21	56.49	40.82 ↑	65.54 ↑
DcNet [7]	39.44	58.89	31.09	54.72
DcNet+RALAD (ours)	39.07	57.64	42.11 ↑	67.24 ↑

TABLE II
TRAINING COST

Methods	KITTI	CARLA
MonoLayout [5]	34.84 s/epoch	33.97 s/epoch
MonoLayout+RALAD	3.81 s/epoch	4.07 s/epoch
Cross_view [6]	41.54 s/epoch	41.33 s/epoch
Cross_view+RALAD	5.27 s/epoch	5.29 s/epoch
DcNet [7]	68.07 s/epoch	67.97 s/epoch
DcNet+RALAD	20.23 s/epoch	21.08 s/epoch

TABLE III
CONVEX COMBINATION OF RATIO SETTING

KITTI:CARLA	Metrics (mIOU/mAP)	
	KITTI	CARLA
0.7:0.3	34.70 / 54.48	22.06 / 47.62
0.6:0.4	32.10 / 54.02	35.12 / 63.33
0.5:0.5	30.21 / 52.83	35.77 / 60.74
0.4:0.6	29.68 / 49.33	36.83 / 61.39

the 0.7:0.3 combination performed better on KITTI (34.70% mIOU, 54.48% mAP) but much worse on CARLA. As the CARLA ratio increased (0.5:0.5 and 0.4:0.6), performance on CARLA continued to improve, reaching the highest metrics with the 0.4:0.6 combination (36.83% mIOU, 61.39% mAP), but at the cost of reduced performance on KITTI. The experiments indicate that as the ratio of CARLA data increases, the model’s performance on CARLA improves significantly, with the best results seen at the 0.4:0.6 ratio. Conversely, the model’s performance on KITTI decreases as the CARLA ratio increases. The experimental data clearly indicates that 0.6:0.4 is an effective ratio, which not only ensures the performance of the model but also demonstrates good robustness and adaptability. Therefore, in our experiments, we recommend and adopt this ratio for feature fusion in order to achieve more outstanding results in experimental results and application value.

V. CONCLUSIONS

In conclusion, our RALAD model has demonstrated remarkable effectiveness in reducing the gap between real and simulated scenarios. By doing so, it not only maintains the high accuracy achieved in real scenes but also significantly improves the detection accuracy in simulated scenarios. This achievement holds great promise for the field of autonomous driving. Looking ahead, we are determined to conduct further experiments with RALAD in other areas of autonomous driving.

REFERENCES

- [1] Dong J, Chen S, Miralinaghi M, et al. Development and testing of an image transformer for explainable autonomous driving systems[J]. *Journal of Intelligent and Connected Vehicles*, 2022, 5(3): 235-249.
- [2] Atakishiyev S, Salameh M, Yao H, et al. Explainable artificial intelligence for autonomous driving: A comprehensive overview and field guide for future research directions[J]. *IEEE Access*, 2024.
- [3] Chib P S, Singh P. Recent advancements in end-to-end autonomous driving using deep learning: A survey[J]. *IEEE Transactions on Intelligent Vehicles*, 2023.
- [4] Cui C, Ma Y, Cao X, et al. A survey on multimodal large language models for autonomous driving[C]//*Proceedings of the IEEE/CVF Winter Conference on Applications of Computer Vision*. 2024: 958-979.
- [5] Mani K, Daga S, Garg S, et al. Monolayout: Amodal scene layout from a single image[C]//*Proceedings of the IEEE/CVF Winter Conference on Applications of Computer Vision*. 2020: 1689-1697.
- [6] Yang W, Li Q, Liu W, et al. Projecting your view attentively: Monocular road scene layout estimation via cross-view transformation[C]//*Proceedings of the IEEE/CVF conference on computer vision and pattern recognition*. 2021: 15536-15545.
- [7] Kim C, Kim U H. A Dual-Cycled Cross-View Transformer Network for Unified Road Layout Estimation and 3D Object Detection in the Bird's-Eye-View[C]//*2023 20th International Conference on Ubiquitous Robots (UR)*. IEEE, 2023: 41-47.
- [8] Alaba S Y, Ball J E. Deep learning-based image 3-d object detection for autonomous driving[J]. *IEEE Sensors Journal*, 2023, 23(4): 3378-3394.
- [9] Wu H, Wen C, Li W, et al. Transformation-equivariant 3d object detection for autonomous driving[C]//*Proceedings of the AAAI Conference on Artificial Intelligence*. 2023, 37(3): 2795-2802.
- [10] Hu Y, Yang J, Chen L, et al. Planning-oriented autonomous driving[C]//*Proceedings of the IEEE/CVF Conference on Computer Vision and Pattern Recognition*. 2023: 17853-17862.
- [11] Geiger A, Lenz P, Stiller C, et al. Vision meets robotics: The kitti dataset[J]. *The International Journal of Robotics Research*, 2013, 32(11): 1231-1237.
- [12] Sun P, Kretschmar H, Dotiwalla X, et al. Scalability in perception for autonomous driving: Waymo open dataset[C]//*Proceedings of the IEEE/CVF conference on computer vision and pattern recognition*. 2020: 2446-2454.
- [13] Caesar H, Bankiti V, Lang A H, et al. nuscenes: A multimodal dataset for autonomous driving[C]//*Proceedings of the IEEE/CVF conference on computer vision and pattern recognition*. 2020: 11621-11631.
- [14] Bolte J A, Bar A, Lipinski D, et al. Towards corner case detection for autonomous driving[C]//*2019 IEEE Intelligent vehicles symposium (IV)*. IEEE, 2019: 438-445.
- [15] Breitenstein J, Termöhlen J A, Lipinski D, et al. Corner cases for visual perception in automated driving: some guidance on detection approaches[J]. *arXiv preprint arXiv:2102.05897*, 2021.
- [16] Li K, Chen K, Wang H, et al. Coda: A real-world road corner case dataset for object detection in autonomous driving[C]//*European Conference on Computer Vision*. Cham: Springer Nature Switzerland, 2022: 406-423.
- [17] Hu X, Li S, Huang T, et al. How simulation helps autonomous driving: A survey of sim2real, digital twins, and parallel intelligence[J]. *IEEE Transactions on Intelligent Vehicles*, 2023.
- [18] Cui Y, Liu Z, Chen Y, et al. Retrieval-augmented multiple instance learning[J]. *Advances in Neural Information Processing Systems*, 2024, 36.
- [19] Mondal A, Tigas P, Gal Y. Real2sim: Automatic generation of open street map towns for autonomous driving benchmarks[C]//*Machine Learning for Autonomous Driving Workshop at the 34th Conference on Neural Information Processing Systems (NeurIPS)*. 2020.
- [20] Xiaozhi Chen, Kaustav Kundu, Ziyu Zhang, Huimin Ma, and Raquel Urtasun. Monocular 3d object detection for autonomous driving. In *CVPR*, 2016.
- [21] Daoud A, Bunel C, Guérliau M. CornerSim: A Virtualization Framework to Generate Realistic Corner-Case Scenarios for Autonomous Driving Perception Testing[J]. *Procedia Computer Science*, 2024, 238: 184-191.
- [22] Shivam Kalra, Hamid R Tizhoosh, Charles Choi, Sultaan Shah, Phedias Diamandis, Clinton JV Campbell, and Liron Pantanowitz. Yottixel—an image search engine for large archives of histopathology whole slide images. *Medical Image Analysis*, 65:101757, 2020.
- [23] Chengkuan Chen, Ming Y Lu, Drew FK Williamson, Tiffany Y Chen, Andrew J Schaumberg, and Faisal Mahmood. Fast and scalable search of whole-slide images via self-supervised deep learning. *Nature Biomedical Engineering*, 6(12):1420–1434, 2022.
- [24] Anna Yeaton, Rahul G Krishnan, Rebecca Mieloszyk, David Alvarez-Melis, and Grace Huynh. Hierarchical optimal transport for comparing histopathology datasets. *arXiv preprint arXiv:2204.08324*, 2022.
- [25] Udupa, Sumanth and Gurunath, Prajwal and Sikdar, Aniruddh and Sundaram, Suresh. MRFP: Learning Generalizable Semantic Segmentation from Sim-2-Real with Multi-Resolution Feature Perturbation. In *CVPR*, 2024.
- [26] A. Kadian et al., “Sim2real predictivity: Does evaluation in simulation predict real-world performance?,” *IEEE Robot. Autom. Lett.*, vol. 5, no. 4, pp. 6670–6677, Oct. 2020.
- [27] X. Hu, S. Li, T. Huang, B. Tang, R. Huai and L. Chen, “How Simulation Helps Autonomous Driving: A Survey of Sim2real, Digital Twins, and Parallel Intelligence,” in *IEEE Transactions on Intelligent Vehicles*, vol. 9, no. 1, pp. 593-612, Jan. 2024
- [28] Xie, Yiming et al. “SynFog: A Photo-realistic Synthetic Fog Dataset based on End-to-end Imaging Simulation for Advancing Real-World Defogging in Autonomous Driving.” *ArXiv abs/2403.17094* (2024): n. pag.
- [29] Marco Cuturi. Sinkhorn distances: Lightspeed computation of optimal transport. *Advances in neural information processing systems*, 26, 2013.